Supporting Information for:

Gravitational Settling Effects on Unit Cell Predictions of Colloidal Retention in Porous Media in the Absence of Energy Barriers

Huilian Ma, Eddy F. Pazmino, William P. Johnson*

Department of Geology and Geophysics

University of Utah, Salt Lake City, UT 84112

Text: 3

Tables: 3

Figures: 6

Total pages: 13

* Corresponding author. E-mail: william.johnson@utah.edu; Tel: (801)581-5033; Fax: (801)585-7065.

Favorable conditions for column experiments

All the experiments were performed under favorable conditions (i.e. in the absence of energy barriers). The favorable conditions were achieved via two strategies: i) using the cleaned glass beads and setting the solution ionic strength to 50 mM and pH to 2.0;[1] and ii) using iron oxide-coated glass beads and setting the solution ionic strength to 1 mM and pH to 6.72.[2] These two strategies were experimentally tested to be equivalent and are not distinguished in the results.[2] The corresponding zeta potentials for some of microspheres used and the glass beads at the experiment conditions were provided in the Table S2.

Trajectory analysis

A Lagrangian approach was used to mechanistically simulate particle trajectories based on the classical Langevin equation:[3]

$$(m + m^*)\frac{du}{dt} = F_D + F_G + F_L + F_{EDL} + F_{vdW} + F_B$$

where m is the particle mass, m^* is the virtual mass (approximated by one-half the displaced fluid volume by the particle), u is the particle velocity vector, and the terms on the right-hand-side of the equation are the forces acting on the particle. These forces include fluid drag (F_D), gravity (F_G), shear lift (F_L), electrostatic (F_{EDL}), van der Waals (F_{vdW}), and Brownian (F_B).

Colloids are introduced to a specified plane located at the upstream side of the modeled domain. Attachment is defined as the separation distance between a colloid and the collector surface is within 1 nm. Colloids leaving the modeled domain (i.e. specified downstream exit plane) are considered exited (no attachment).

Comparisons between Happel sphere-in-cell and hemispheres-in-cell models

The hemispheres-in-cell model and Happel sphere-in-cell model share attributes such as adjustable porosity via changing the thickness of the fluid envelope relative to collector size; and an outer fluid boundary which acts as a "watershed" divide (non-tangential stress boundary) among adjacent collectors. The hemispheres-in-cell model differs from the Happel model in that the former contains a grain to grain contact, which has been shown to be important in colloidal retention in porous media under unfavorable conditions (i.e. presence of energy barriers).[4, 5]

Boundary conditions in both models include no-slip boundaries at grain surfaces, non-tangential stress at the fluid envelope outer boundaries, and stipulations on velocity (or pressure) at the cell entry and exit planes.[3]

Literature cited:

1. Tong, M.; Johnson, W. P. Excess colloid retention in porous media as a function of colloid size, fluid velocity, and grain angularity. *Environ. Sci. Technol.* **2006,** *40*(24), 7725-7731.

2. Pazmino, E.; Ma, H.; Johnson, W. P. Applicability of colloid filtration theory in size-distributed, reduced porosity, granular media in the absence of energy barriers. *Environ. Sci. Technol.***,** in review.

3. Ma, H.; Pedel, J.; Fife, P.; Johnson, W. P. Hemispheres-in-cell geometry to predict colloid deposition in porous media. *Environ. Sci. Technol.* **2009,** *43*(22), 8573-8579.

4. Bradford, S. A.; Bettahar, M. Straining, attachment, and detachment of Cryptosporidium oocysts in saturated porous media. *J. Environ. Quality* **2005,** *34*(2), 469-478.

5. Johnson, W. P.; Li, X.; Yal, G. Colloid retention in porous media: Mechanistic confirmation of wedging and retention in zones of flow stagnation. *Environ. Sci. Technol.* **2007,** *41*(4), 1279-1287.

6. Li, X.; Scheibe, T. D.; Johnson, W. P., Apparent decreases in colloid deposition rate coefficients with distance of transport under unfavorable deposition conditions: A general phenomenon. *Environ. Sci. Technol.* **2004,** *38*(21), 5616-5625.

Table S1. Parameters Used in the Simulation and Experiment

parameter	simulation	experiment		
collector diameter, d_c (μm)	510	147-850;	740-800;	510;
porosity, ε	0.25; 0.37	0.28;	0.34;	0.38;
pore water velocity, v_p (m/day)	4, 40	4	3.3	3
colloid diameter, d_p (μm)	0.04 - 10	0.21, 0.5, 1.1, 2.0, 4.4, 9.0		
colloid density, ρ_p (g/cm^3)	1.055, 4.0	1.055		
fluid density, ρ_f (g/cm^3)	0.998	0.998		
fluid viscosity, μ (kg · m/s)	9.98×10^{-4}	9.98×10^{-4}		
Hamaker constant, A (J)	3.84×10^{-21}	3.84×10^{-21}		
absolute temperature, T (K)	298.2	298.2		
ionic strength (mM)	1	50		
pH	----	2		
colloid zeta potential, (mV)	-20	-2.3, -5.2, -6, -5.4, -8, -10		
collector zeta potential, (mV)	60	-10		

Table S2. Zeta-potential for microspheres and crushed glass collector at pH = 2 and ionic strength of 50mM.[1, 6] Favorable conditions for deposition were achieved under this experimental condition. The potential energy profiles as a function of separation distance from DLVO theory are plotted in Figure S1 based on these zeta potential values; and please refer to Tong et al. [1] for DLVO force expressions and parameters.

Particles		Zeta potential (mV)	
		pH	Ionic strength (50 mM)
Carboxylate-modified microspheres (μm)	0.21	2	-2.3 ± 0.49
	0.5	2	-5.2 ± 0.98
	1.1	2	-6.0 ± 0.55
	2.0	2	-5.4 ± 0.81
	4.4	2	-8.0 ± 0.41
	9.1	2	-10.0 ± 0.5
Crushed collector	Glass beads	2	-10.0 ± 1.85

Table S3. Relative magnitude of fluid drag, gravity and diffusion forces under simulated and experimental conditions.

	averaged pore water velocity (m/day)		colloid density (g/cm^3)		colloid density (g/cm^3)	
	4	40	1.055	4	1.055	4
colloid diameter (μm)	fluid drag forces (N)		gravitational forces (N)		Brownian forces (N)*	
0.04	1.74E-14	1.74E-13	1.87E-20	9.87E-19	4.79E-13	2.46E-13
0.1	4.35E-14	4.35E-13	2.93E-19	1.54E-17	3.03E-13	1.56E-13
0.21	9.14E-14	9.14E-13	2.71E-18	1.43E-16	2.09E-13	1.07E-13
0.4	1.74E-13	1.74E-12	1.87E-17	9.87E-16	1.51E-13	7.78E-14
0.5	2.18E-13	2.18E-12	3.66E-17	1.93E-15	1.35E-13	6.95E-14
0.6	2.61E-13	2.61E-12	6.32E-17	3.33E-15	1.24E-13	6.35E-14
0.8	3.48E-13	3.48E-12	1.50E-16	7.89E-15	1.07E-13	5.50E-14
1	4.35E-13	4.35E-12	2.93E-16	1.54E-14	9.58E-14	4.92E-14
1.1	4.79E-13	4.79E-12	3.90E-16	2.05E-14	9.13E-14	4.69E-14
1.6	6.97E-13	6.97E-12	1.20E-15	6.32E-14	7.57E-14	3.89E-14
2	8.71E-13	8.71E-12	2.34E-15	1.23E-13	6.77E-14	3.48E-14
3	1.31E-12	1.31E-11	7.91E-15	4.16E-13	5.53E-14	2.84E-14
4	1.74E-12	1.74E-11	1.87E-14	9.87E-13	4.79E-14	2.46E-14
4.4	1.92E-12	1.92E-11	2.49E-14	1.31E-12	4.57E-14	2.34E-14
5	2.18E-12	2.18E-11	3.66E-14	1.93E-12	4.28E-14	2.20E-14
6	2.61E-12	2.61E-11	6.32E-14	3.33E-12	3.91E-14	2.01E-14
7	3.05E-12	3.05E-11	1.00E-13	5.29E-12	3.62E-14	1.86E-14
8	3.48E-12	3.48E-11	1.50E-13	7.89E-12	3.39E-14	1.74E-14
9.1	3.96E-12	3.96E-11	2.21E-13	1.16E-11	3.17E-14	1.63E-14
10	4.35E-12	4.35E-11	2.93E-13	1.54E-11	3.03E-14	1.56E-14

Note: the fluid drag forces are calculated based on the averaged pore water velocity (v_p), according to $6\pi\mu a_p v_p$, where μ is fluid viscosity, and a_p is the colloid radius.

The Brownian forces are computed based on

$$F_B = \Re\sqrt{\frac{2\xi kT}{\Delta t}}$$

where $\Re$ is a Gaussian random number with zero mean and unit variance; k is the Boltzmann constant; T is the absolute temperature; and ξ is the friction coefficient (= $6\pi\mu a_p$), and $\Delta t = m/\xi$. Due to their randomness in nature, we strongly suggest not to take their face values to compare to fluid drag and gravity forces.

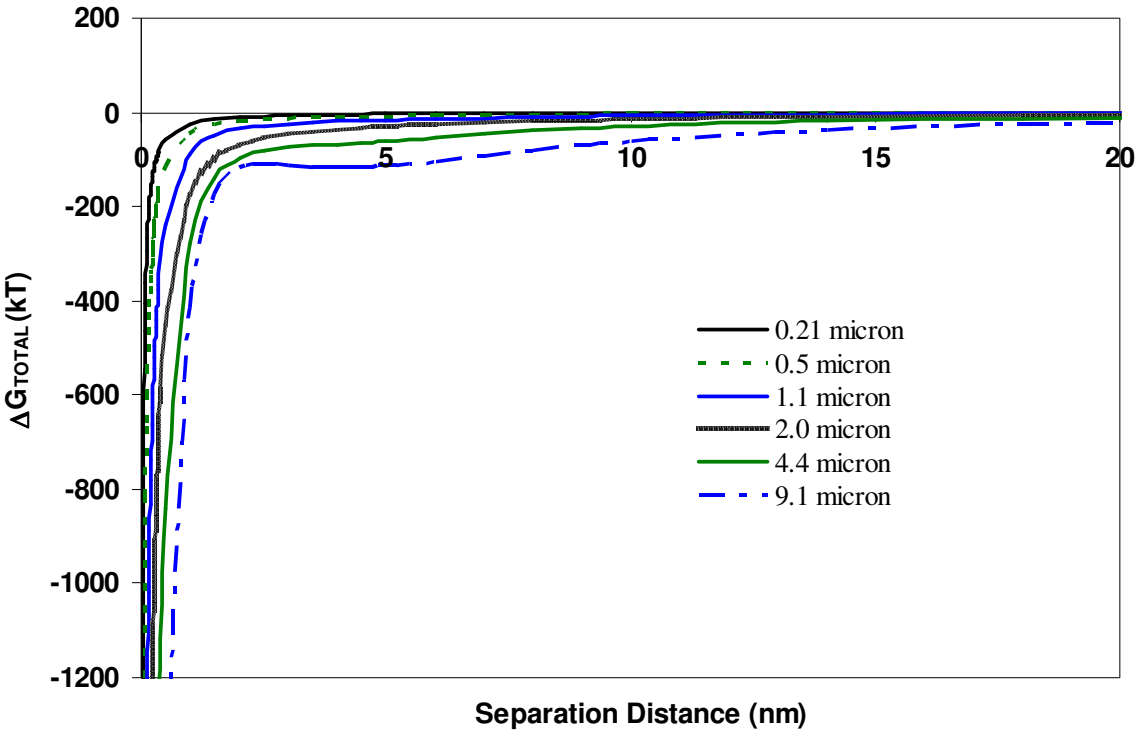

FIGURE S1. Potential energy calculated from DLVO theory a function of separation distance for different colloid size using zeta potential values from Table S1. The absence of energy barriers indicates favorable conditions are achieved.

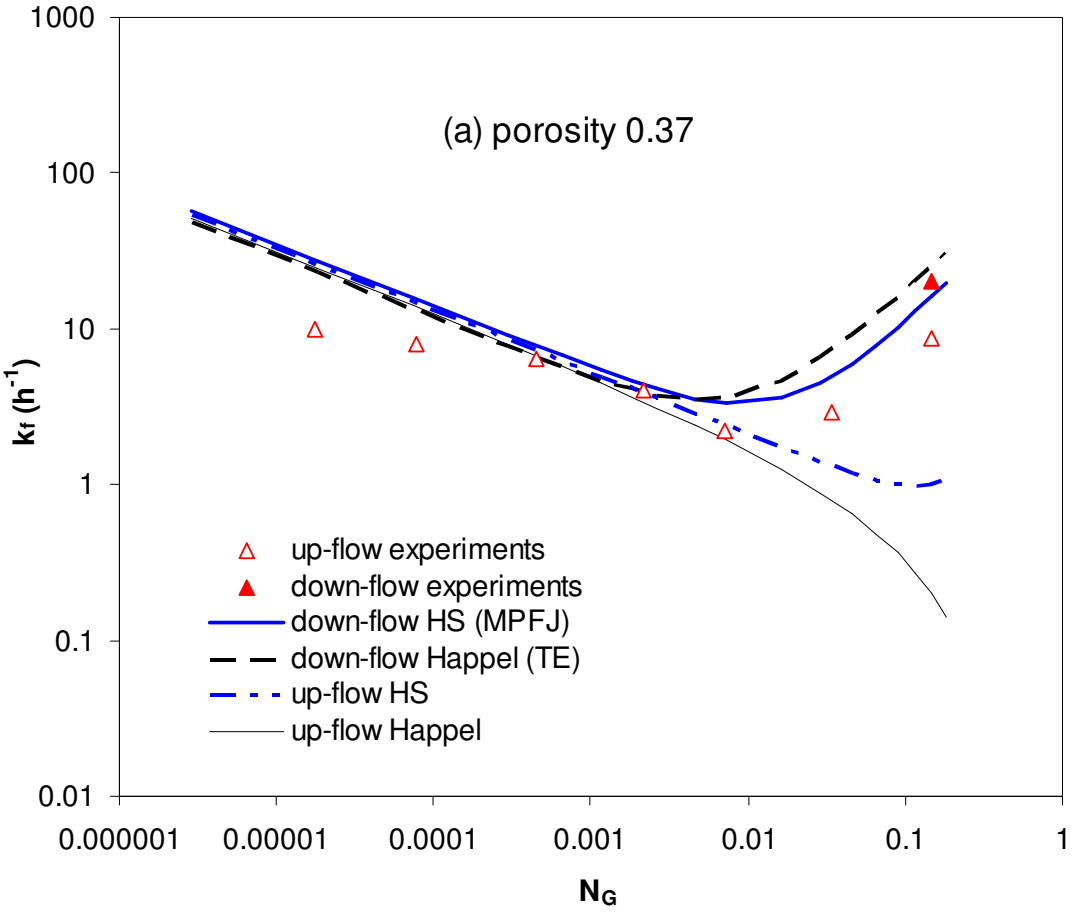

FIGURE S2. Re-plotting of Figure 2a from the manuscript as a function of N_G.

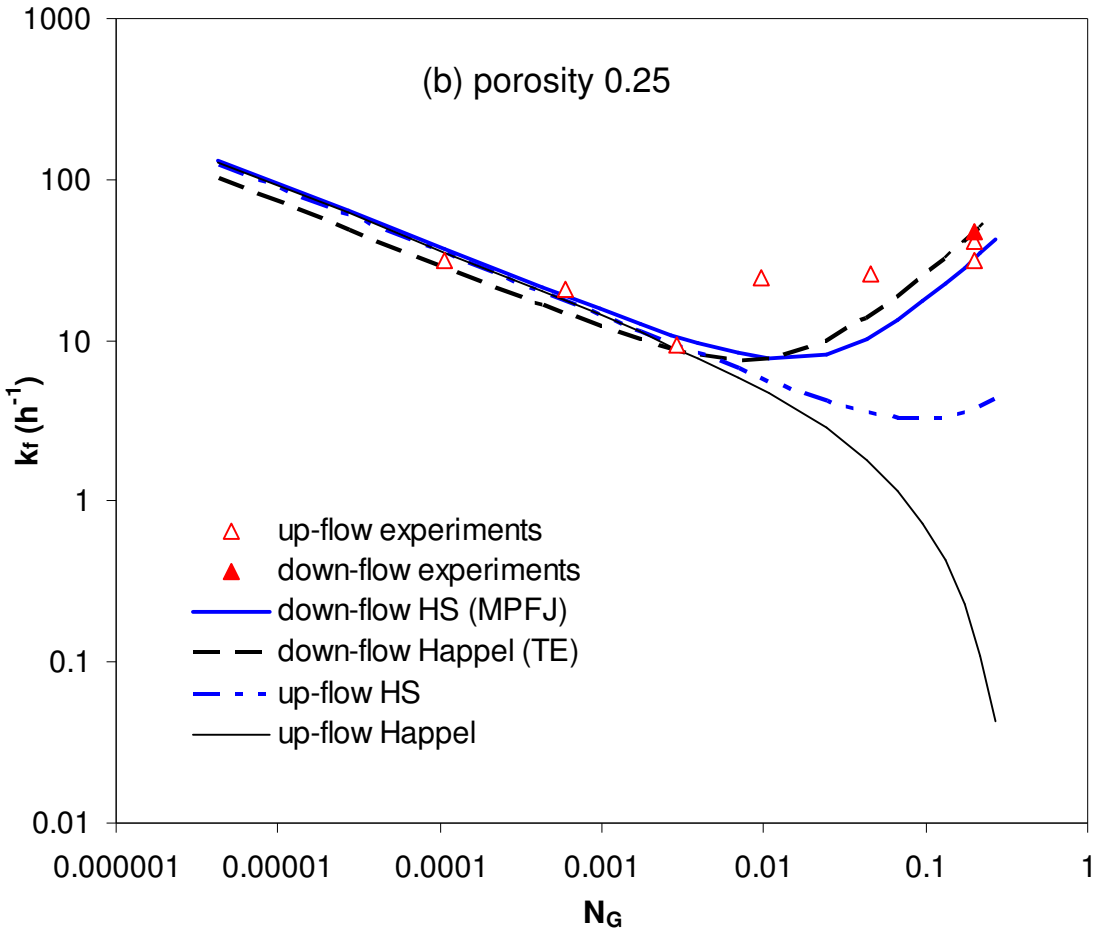

FIGURE S3. Re-plotting of Figure 2b from the manuscript as a function of N_G.

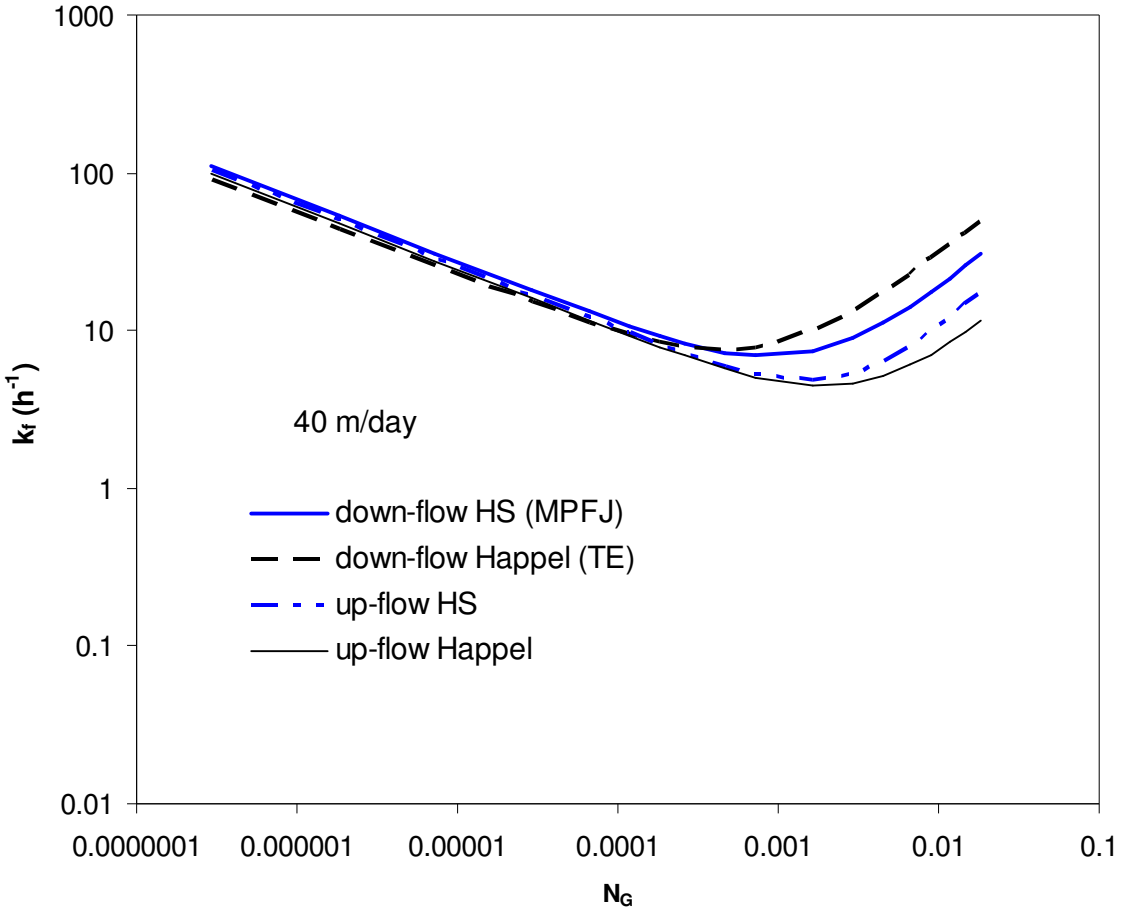

FIGURE S4. Re-plotting of Figure 4 from the manuscript as a function of N_G.

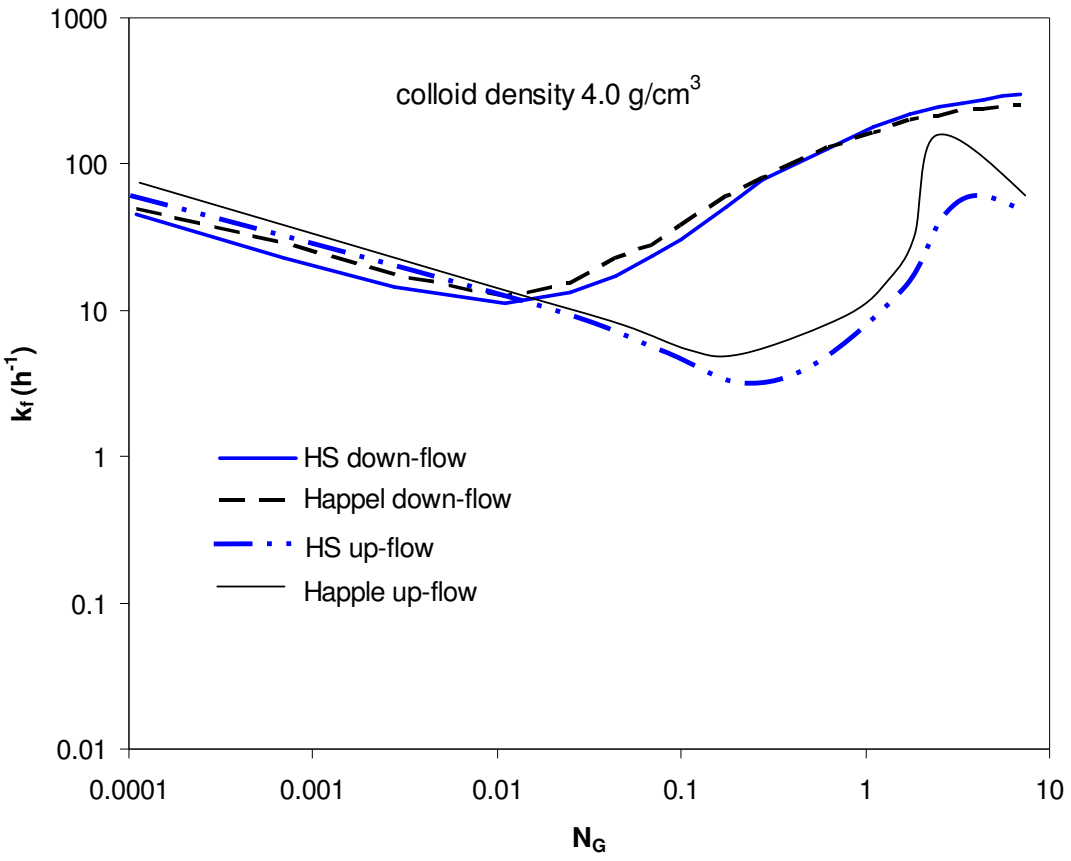

FIGURE S5. Re-plotting of Figure 6 from the manuscript as a function of N_G. Note that k_f values dropping to 0 for large N_G (or large size colloids) are not illustrated here, as in Figure 6.

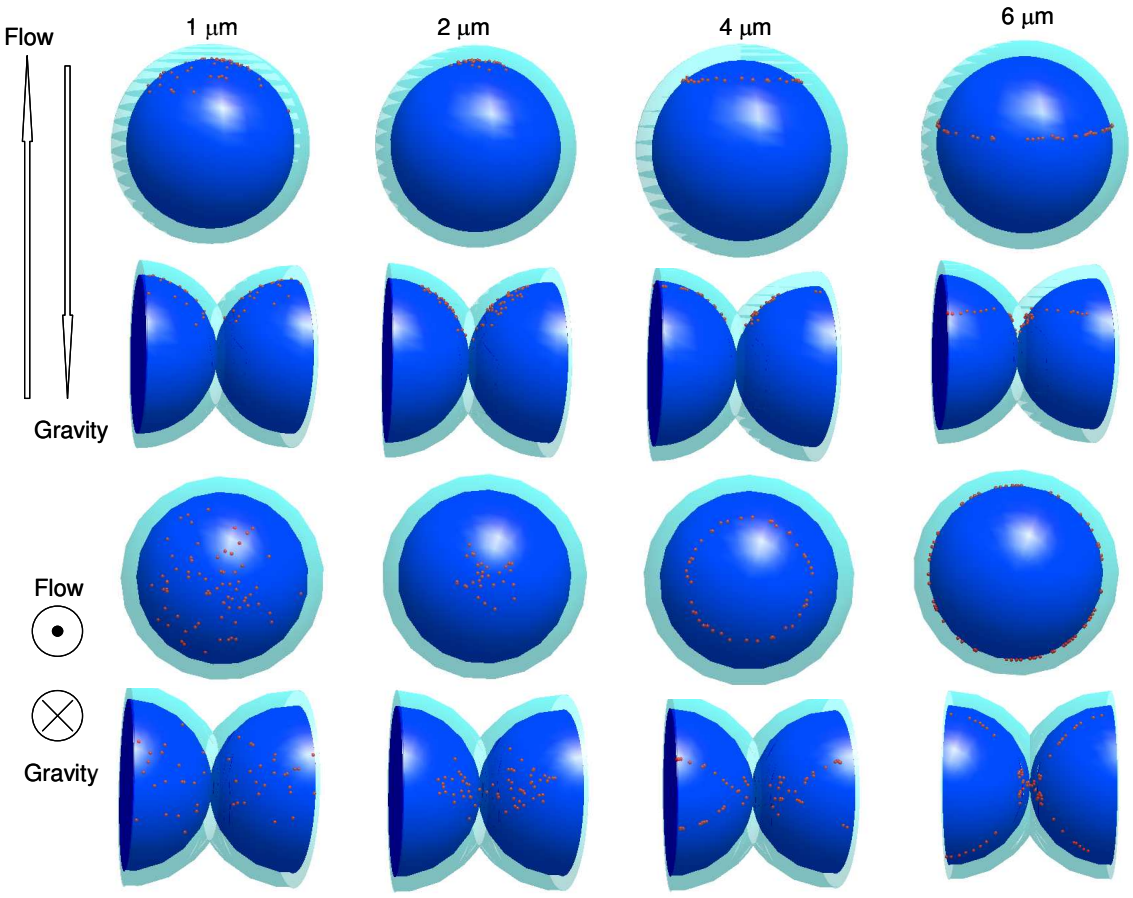

FIGURE S6. Locations of deposited colloids (density 4.0 g/cm^3) of four representative sizes (1, 2, 4 and 6 μm) onto the two unit cell collector surfaces under up-flow conditions at porosity 0.37 and pore water velocity 4 m/day, for simulations presented in Figure 6 in the manuscript. The top two rows are side views for the Happel and hemispheres-in-cell (HS) models, respectively. The bottom two rows are top views for Happel and HS models, respectively. The colloid size labels apply to the whole column.